# Quasiperiodicity and Chaos in a System with Three Competing Frequencies

Andrew Cumming and Paul S. Linsay
*Department of Physics, Massachusetts Institute of Technology, Cambridge, Massachusetts 02139*
(Received 4 April 1988)

We present measurements of the phase diagram for a nonlinear electronic oscillator circuit which has three intrinsic frequencies. The persistence of chaos to almost zero intermode coupling and the measured structure of the chaotic zones in parameter space provide unprecedented detail in the interpretation of the Ruelle-Takens scenario for the onset of chaos.

PACS numbers: 05.45.+b, 03.40.−t, 05.40.+j

There has been a great deal of interest in the past decade in the transition to chaos in systems with a small number of intrinsic frequencies. To set the stage, we recall that the Landau[1] picture of the onset of turbulence in fluid systems involved a succession of an infinite number of Hopf bifurcations, each of which introduced a new, generally incommensurate frequency to the problem. This view was supplanted by the work of Ruelle and Takens[2] (RT) and later that of Newhouse, Ruelle, and Takens,[3] who proved that with as few as three independent frequencies in a dynamical system, three-frequency quasiperiodic flows are structurally unstable to the development of a strange attractor. This means that an arbitrarily small perturbation in parameter value causes a system undergoing three-frequency quasiperiodic flow to become chaotic. RT went on to speculate on this being the mechanism for the onset of turbulence in systems with many degrees of freedom.

Experimental work in the ensuing years served neither to confirm the theory nor refute it because some experiments demonstrated the onset of chaos after the introduction of the third frequency,[4] while others allowed the nonchaotic inclusion of three or more incommensurate frequencies.[5] Grebogi, Ott, and Yorke[6] showed in numerical experiments on a simple torus map system that a reasonable interpretation of these seemingly conflicting results is that though three-frequency quasiperiodicity may be structurally unstable, chaos is unlikely in a measure-theoretic sense, especially for small values of the nonlinear coupling parameter. They published some low-resolution parameter-space phase diagrams which confirmed their hypothesis, but left some question as to the exact structure of the chaotic region in the parameter space.

Attracting flows on the three-torus are best characterized by the definition of two winding numbers from the system's frequencies, $\omega_0$, $\omega_1$, and $\omega_2$:

$$\rho_1=\omega_1/\omega_0, \quad \rho_2=\omega_2/\omega_0.$$

Clearly if neither $\rho_1$ nor $\rho_2$ can be written as a rational number $p/q$ with $p$ and $q$ integers, and $\rho_1/\rho_2$ is not rational, then all three frequencies are incommensurate and the flow is said to be three-frequency quasiperiodic. If

$$\rho_1=p/q+\rho_2 r/s, \quad \{p,q,r,s\}\in\mathbb{Z},$$

then two of the modes are locked together, and there is two-frequency quasiperodicity.[7] If all frequencies are locked into rational ratios, then the motion is periodic. The fourth possibility is that of a strange attractor,[8] which requires at least a three-dimensional phase space given the constraints that nearby trajectories diverge exponentially yet never cross, all the while the motion remaining bounded.

The method of measuring a phase diagram consists of varying the parameters of the problem in some systematic way and, for each parameter-space point, characterizing the flow there. We have devised an experiment which allows us to do just that. Using a pair of operational amplifier relaxation oscillators,[9] symmetrically coupled to each other and to an external drive (Fig. 1), we can adjust all the relevant parameters of the system in a controlled manner. The strong dissipation of the relaxation oscillators ensures that the motion is constrained to the three-torus for low drive amplitudes relative to the characteristic amplitudes of the oscillators themselves. The operational amplifiers operate from stabilized $\pm 5$-V supplies, which along with the ratio of the coupling capacitance to the oscillator capacitance $C_c/C_{\rm osc}$ establishes the drive-amplitude scale of the apparatus. The coupling resistance $R_c$ is a relevant parameter, but, in the interest of our keeping the dimensionality of parameter space to three in lieu of the less manageable four, is set to a low value. $R_c$ is chosen such that the characteristic coupling amplitude between oscillators is less than 1% of the drive-amplitude scale. With the $O_1$ free-running (decoupled) frequency set at an arbitrary value of about 250 kHz ($=1/2.2R^1_{\rm osc}C^1_{\rm osc}$), there remain three parameters: the free-running frequency of $O_2$, and the frequency and amplitude of the sinusoidal drive voltage.

Data are encoded by our passing the output from the summing amplifier through a 500-kHz low-pass filter to a fast twelve-bit analog-to-digital converter (ADC). The discrete time series (up to 32768 elements long) is tem-

 

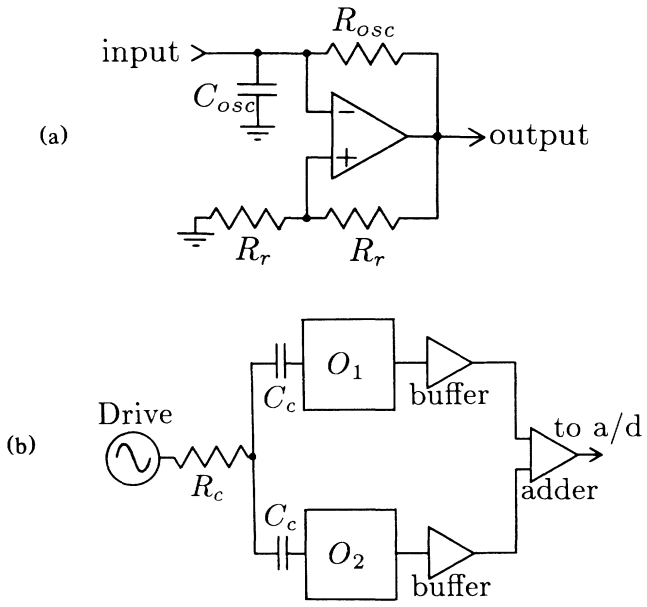


FIG. 1. Circuit used in measurement of three-torus phase diagram. $O_1$ and $O_2$ in (b) are shorthand for the operational amplifier relaxation oscillator in (a), while a/d denotes the ADC. The frequency of $O_2$ can be programmed remotely.

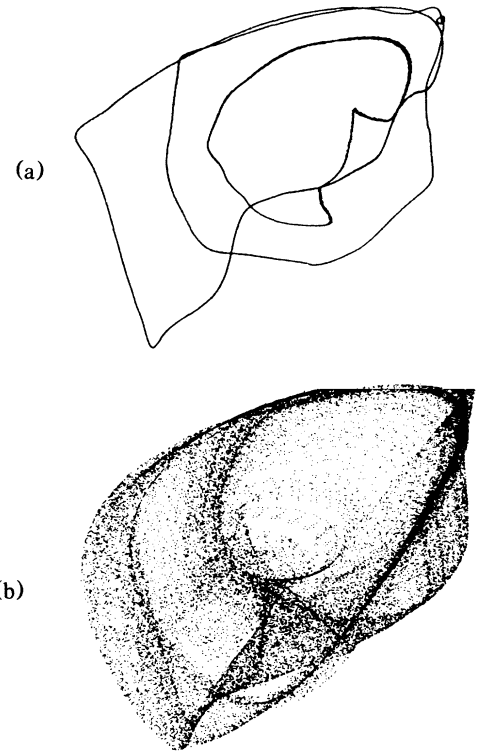


FIG. 2. Projections of the Poincaré sections for typical (a) two-frequency and (b) three-frequency attractors in the reconstructed $V_i$ vs $V_{i+1}$ phase space. The three-frequency attractor lies on a two-dimensional projection of a complicated surface embedded in three space.

porarily stored in a fast buffer memory and is loaded into a computer for further processing. The ADC is triggered by the synchronization signal from a Hewlett-Packard model 3325A signal generator which drives the circuit. The synchronization is a square wave of the same frequency and phase as the drive signal. This ensures that when the attractor is reconstructed from the time series by the plot of adjacent elements as ordered pairs in the $V_i$ vs $V_{i+1}$ phase space, we have a two-dimensional projection of the Pincaré section. The filter serves to soften the corners in the summed signal which occur by virtue of the switched character of the output of the relaxation oscillators. The cutoff frequency is sufficiently high that there is no attractor dimension enhancement of the sort reported by Badii *et al.*[10] Attractors for typical two-frequency and three-frequency orbits are depicted in Figs. 2(a) and 2(b).

Figures 3(a)–3(d) show successively higher-resolution scans in drive amplitude and frequency. Chaos is distinguished from quasiperiodicity in the on-line parameter-space scans by evaluation of the temporal decay of the envelope of the time series autocorrelation function.[11] The chaotic regions persist and have a complicated striated structure at drive amplitudes of less than 1% of the characteristic drive amplitude scale of 8 volts or so. The autocorrelation functions shown in Figs. 4(a) and 4(b) clearly show the sensitivity of this discriminant between chaos and quasiperiodicity.

The results reported here help to clarify the discrepancy between earlier experimental results concerning the onset of chaos on the three-torus. Clearly there is little that can be done in a fluid system, or in higher degree of freedom systems generally, to affect the strength of the coupling between the modes as they are introduced into the dynamics. Consequently, we interpret the experiments which "confirm" the RT scenario as those whose parameters have accidentally fallen on chaotic regions of the phase diagram, while those which "refute" it to have taken place with the wrong parameters, and indeed most likely those corresponding to low coupling strengths. The phase diagrams included here graphically elucidate what we feel to be the correct interpretation of the RT scenario, by showing the variation in the likelihood and structure of chaos on the three-torus as a function of system parameters for a real physical system.

The majority of parameter space seems to correspond to three-frequency quasiperiodic flow, especially at low values of the coupling, which in our case is the drive amplitude. This is evident in Fig. 3(a) and is consistent with the results of Ref. 6. We emphasize that the squares corresponding to chaos in the lower right half of Fig. 3(a) are not noise. There are countless chaotic bands in this area, but they are too narrow to be found consistently at this low resolution. In those regions

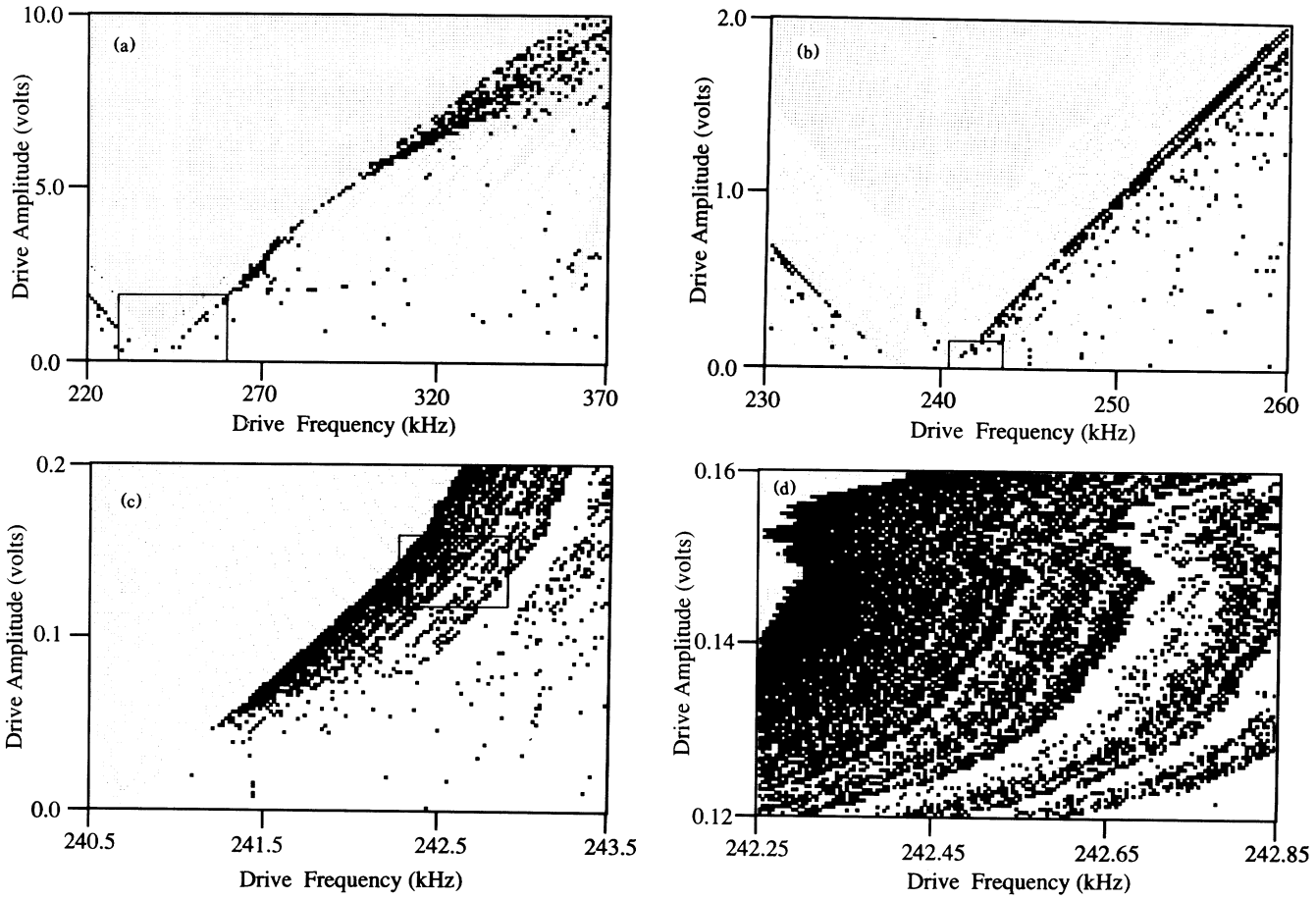


FIG. 3. Drive-amplitude vs drive-frequency phase diagrams at successively higher resolution for the dynamics on the three-torus. The frequency of $O_2$ has been set so that for zero drive amplitude, $O_1$ and $O_2$ are not mode locked. The small boxes in (a)–(c) indicate which portion is magnified in the next figure. Points at which the motion is periodic are represented as dots, and the white regions are quasiperiodic. The black squares represent chaos as determined by an on-line time-series autocorrelation-function criterion. Generally, the white regions which contain the dense scatter of periodic points are two-frequency quasiperiodicity. The clear white areas correspond to alternating bands of two- and three-frequency quasiperiodicity, except in (d) where they are all two-frequency quasiperiodicity.

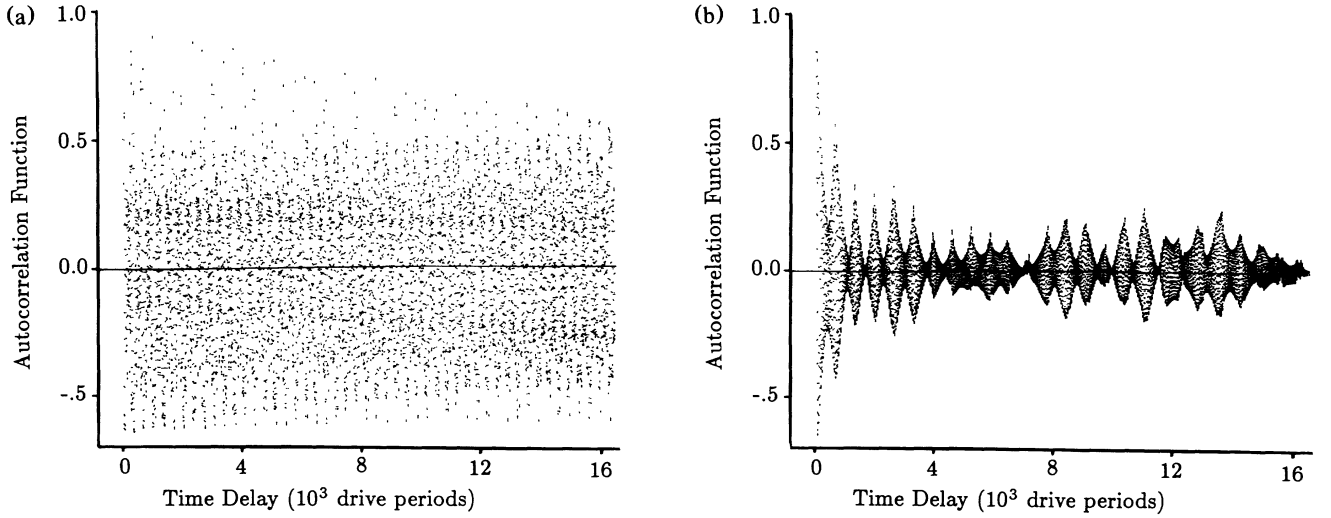


FIG. 4. Digital time-series autocorrelation functions for (a) quasiperiodic and (b) chaotic signals, showing the difference in the speed with which the envelope decays for these two types of behavior.

where chaos is likely at low drive amplitude, such as the one scanned at high resolution in Fig. 3(d), the fact that the chaotic zones occur only at the boundaries of two-frequency quasiperiodic zones suggests the possibility of an experimental "proof" of the structural instability of three-frequency orbits. If one could show that between each pair of two-frequency zones, each of which is flanked by finite width chaotic zones, there is an infinitude of similar structures, then we could conclude that the three-frequency quasiperiodicity is structurally unstable, while the chaos is stable. This would constitute an complete experimental verification of the RT scenario. Although the results reported in this Letter are suggestive of this interpretation, without the guidance afforded by a more fully developed theoretical picture of the problem it is impossible to know what features of this topologically complex situation should be measured. Kim, Mackay, and Guckenheimer[12] have done some interesting numerical work on the properties of the resonance regions for torus maps, though we have yet to observe the phenomena they report. We are, however, now in a position to make use of a scaling theory or phenomenology for the sort of chaotic regions observed experimentally and look forward to its development.

One of us (A.C.) would like to thank Yves Pomeau for helping to motivate the current research. We would also like to thank John Marko, Jim Yorke, and Stéphane Zaleski for useful discussions. This work was supported by the U.S. Office of Naval Research.

[1]L. Landau and E. Lifshitz, *Fluid Mechanics* (Pergamon, Oxford, 1959).

[2]D. Ruelle and F. Takens, Commun. Math. Phys. **20**, 167 (1971).

[3]S. Newhouse, D. Ruelle, and F. Takens, Commun. Math. Phys. **64**, 35 (1978).

[4]Some recent examples are A. Brandtl, T. Geisel, and W. Prettl, Europhys. Lett. **3**, 401 (1987); C. Van Atta and M. Gharib, J. Fluid Mech. **174**, 113 (1987); A. Kourta *et al.*, J. Fluid Mech. **181**, 141 (1987).

[5]See, for example, J. Gollub and S. Benson, J. Fluid Mech. **100**, 449 (1980); R. Walden *et al.*, Phys. Rev. Lett. **53**, 242 (1984).

[6]C. Grebogi, E. Ott, and J. Yorke, Phys. Rev. Lett. **51**, 339 (1983), and Physica (Amsterdam) **15D**, 354 (1985).

[7]K. Kaneko, *Collapse of Tori and Genesis of Chaos in Dissipative Systems* (World Scientific, Singapore, 1986).

[8]See, for instance, P. Bergé, Y. Pomeau, and C. Vidal, *Order Within Chaos* (Wiley, New York, 1986).

[9]P. Horowitz and W. Hill, *The Art of Electronics* (Cambridge Univ. Press, Cambridge, England, 1980).

[10]R. Badii *et al.*, Phys. Rev. Lett. **60**, 979 (1988).

[11]J.-P. Eckmann, Rev. Mod. Phys. **53**, 643 (1981).

[12]S. Kim, R. Mackay, and J. Guckenheimer, Cornell University, Mathematical Science Institute, MSI Technical Report No. 88-9, 1988 (unpublished).

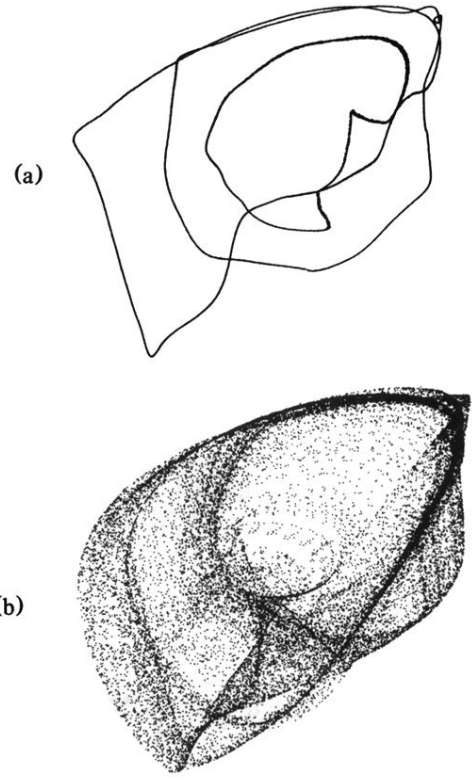


FIG. 2. Projections of the Poincaré sections for typical (a) two-frequency and (b) three-frequency attractors in the reconstructed $V_i$ vs $V_{i+1}$ phase space. The three-frequency attractor lies on a two-dimensional projection of a complicated surface embedded in three space.

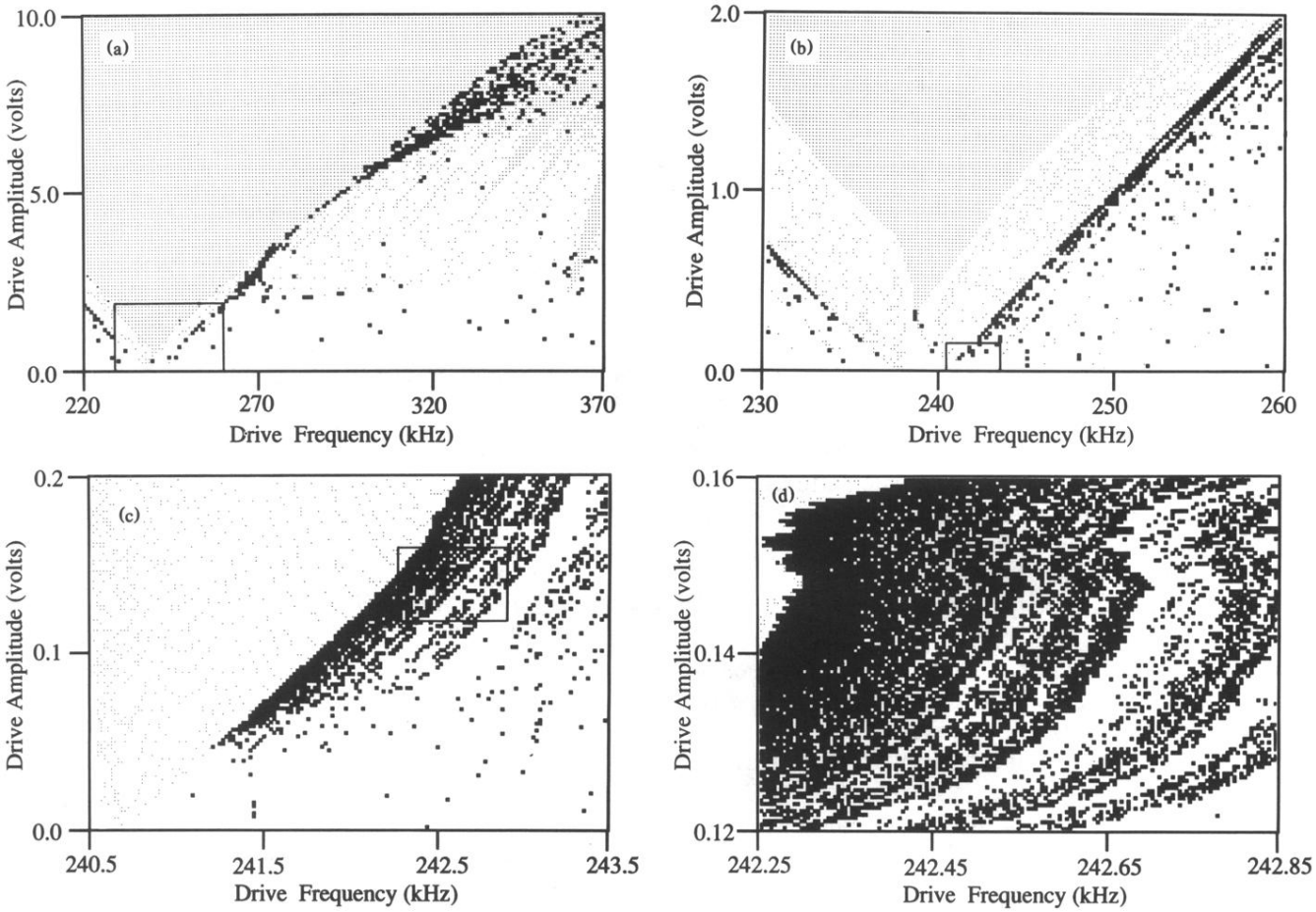


FIG. 3. Drive-amplitude vs drive-frequency phase diagrams at successively higher resolution for the dynamics on the three-torus. The frequency of $O_2$ has been set so that for zero drive amplitude, $O_1$ and $O_2$ are not mode locked. The small boxes in (a)–(c) indicate which portion is magnified in the next figure. Points at which the motion is periodic are represented as dots, and the white regions are quasiperiodic. The black squares represent chaos as determined by an on-line time-series autocorrelation-function criterion. Generally, the white regions which contain the dense scatter of periodic points are two-frequency quasiperiodicity. The clear white areas correspond to alternating bands of two- and three-frequency quasiperiodicity, except in (d) where they are all two-frequency quasiperiodicity.

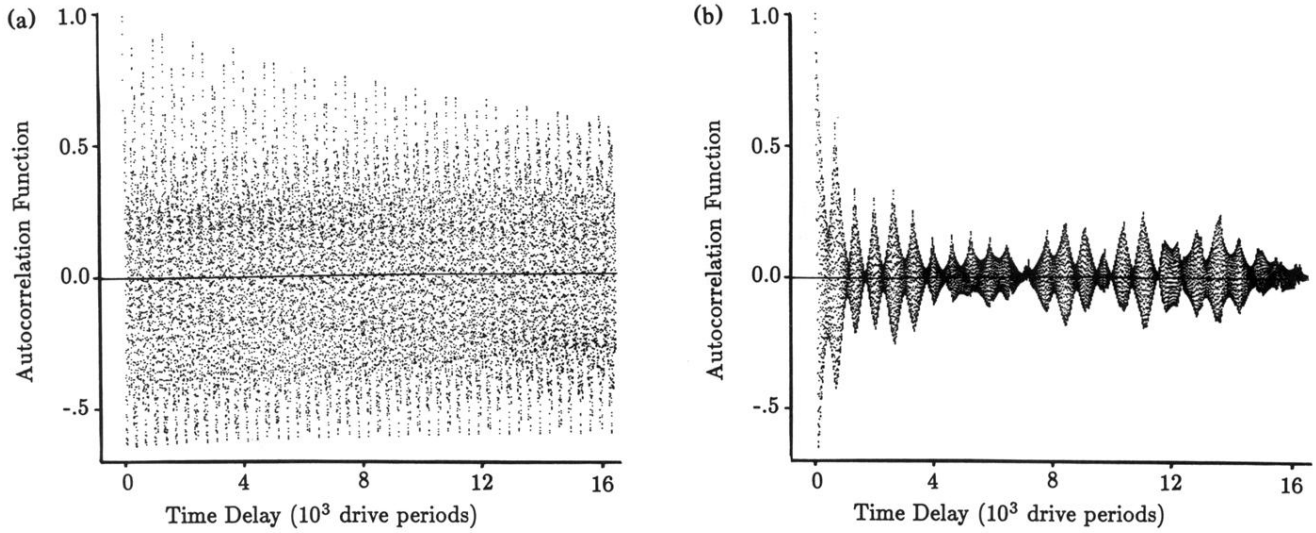


FIG. 4. Digital time-series autocorrelation functions for (a) quasiperiodic and (b) chaotic signals, showing the difference in the speed with which the envelope decays for these two types of behavior.